Marine Environmental Research 183 (2023) 105825

Contents lists available at ScienceDirect

Marine Environmental Research

journal homepage: www.elsevier.com/locate/marenvrev

Spatiotemporal dynamics analysis of aquaculture zones and its impact on green tide disaster in Haizhou Bay, China

Bo Ai, Peipei Wang *, Zhengyi Yang, Yuxin Tian, Dandan Liu

College of Geodesy and Geomatics, Shandong University of Science and Technology, Qingdao, 266590, China

ARTICLE INFO

Keywords:
Mariculture area
Object-oriented
Spatiotemporal dynamics
Driving force
Enteromorpha prolifera
Haizhou bay

ABSTRACT

With the rapid marine economic development, the problem of the marine ecological environment has become progressively prominent. Mariculture monitoring plays an essential role in sustaining ecological stability, rational planning, and green economic development of sea areas. Using the Landsat image, the raft-mariculture area information of Haizhou Bay and its adjacent southern waters were extracted by the object-oriented classification method based on remote sensing techniques. Landscape pattern index and principal component analysis were used to analyze the spatiotemporal expansion and structural changes of mariculture areas, and to quantify the effects of natural, socio-economic factors on the spatiotemporal variations of mariculture areas. This study discusses the correlation between the mariculture area and the outbreak scale of Enteromorpha Enteromorpha green tide. Results show that the object-oriented classification method has the highest accuracy, with total classification accuracy and Kappa coefficient of more than 90% and 0.79, respectively. The total area, patch density, and landscape shape index of mariculture areas in Haizhou Bay increase yearly, which demonstrates that the heterogeneity and fragmentation increase with the expansion of the mariculture area. The landscape pattern changes in the mariculture area are predominantly impacted by annual mean sea surface temperature (SST), annual average wind speed, social development level, and population density, etc. The larger the area of raft-aquaculture, the wider the outbreak scale of the Enteromorpha prolifera disaster. Study results can provide scientific references for the further development of mariculture in Haizhou Bay and marine environmental protection.

1. Introduction

In recent years, the demand for aquatic products in domestic and foreign markets has increased sharply, and mariculture industry has also thrived (Zou and Huang, 2015; Engle, 2016; Nadarajah and Flaaten, 2017). While mariculture creates substantial economic benefits for the country and its people, it has also put more pressure on the coastal ecosystem. The State Council of China issued central document No.1 "*opinions on speeding up the green development of aquaculture*" in 2020, which states that all departments should promote advanced and applicable green aquaculture technology. The green development of aquaculture should be accelerated while protecting the marine environment (Agriculture Fisheries Bureau, 2019). Recently, marine water environmental pollution has occurred frequently, and has resulted in the frequent occurrence of water eutrophication and outbreak of green tide. People have gradually realized that aquaculture development is at the expense of the environment (Boyd et al., 2020; Chen and Chen, 2020b). As aquaculture plays a significant role in the sustainable development of the mariculture industry, it is important to effectively monitor the mariculture area, master the spatiotemporal dynamic change information and explore the influencing factors of the mariculture area change.

In recent years, extensive research attention has been focused on the spatiotemporal dynamic change and influencing factors of coastal ecosystem aquaculture areas. The dynamic monitoring of aquaculture areas is mainly divided into traditional sea area investigation and remote sensing monitoring. Traditional sea area survey is challenging to realize real-time monitoring, which is time-consuming and laborious, and the accuracy is relatively low. That goes against improving aquaculture output and preventing marine disasters (Kang et al., 2019; Wen et al., 2021). Remote sensing technology has various advantages, including a wide monitoring range, fast speed, low cost, and easy long-term dynamic monitoring. It can realize large-scale, efficient, and

* Corresponding author.
E-mail addresses: aibo@sdust.edu.cn (B. Ai), 202083020074@sdust.edu.cn (P. Wang), sdyoung997@163.com (Z. Yang), tianyuxin@sdust.edu.cn (Y. Tian), 202182020038@sdust.edu.cn (D. Liu).

https://doi.org/10.1016/j.marenvres.2022.105825
Received 2 July 2022; Received in revised form 11 November 2022; Accepted 12 November 2022
Available online 14 November 2022

continuous environmental dynamic monitoring (Blondeau-Patissier et al., 2014; Chen et al., 2020). Lu et al. (2015) established the characteristic spectral index for detecting offshore aquaculture areas using Rapideye multispectral images. The high-precision automatic extraction of offshore aquaculture areas was realized. Liu et al. (2020a) brought up an extraction method for the mariculture area based on multi-source feature fusion, including antinormalized difference water index (nNDWI) and green/red (G/R) band ratio, which significantly improved the classification accuracy. Moreover, the spatiotemporal evolution of mariculture areas is affected by multiple driving factors. Chen (2021) applied the random forest algorithm to the quantitative study of multiple influencing factors to analyze the driving mechanism of marine land in Sansha Bay. Ying et al. (2020) studied the long-term landscape changes caused by aquaculture in the coastal area of Ningde city and then discussed its driving factors.

Many researchers use high-resolution images to extract small areas with high precision (Fan et al., 2018; Proisy et al., 2018; B. Cui et al., 2019a; Yan et al., 2021). However, when we conduct real-time monitoring over large areas for a long time, specific problems exist, such as the high cost of high-resolution images and lack of data in some years. In addition, the existing literature seldom attempts to systematically and comprehensively analyze spatiotemporal dynamic changes and their driving forces in coastal aquaculture areas. According to statistics, the raft-aquaculture area in China's coastal zone in 2018 was 194110 ha. The province with the largest area of raft-aquaculture is Jiangsu, accounting for 28.77% (Liu et al., 2020b). Lianyungang has a coastline of more than 170 km, and the curved coastline forms the famous Haizhou Bay. Many mariculture areas in Jiangsu Province are located in Haizhou Bay, Lianyungang City, and Jiangsu Province, China (Zhang et al., 2013). In the past 30 years, Lianyungang's marine economy has continuously transformed from a traditional marine industry to a newly emerging one. The continuous promotion of the modern marine industry has comprehensively accelerated the development of marine fisheries (Journal of the history of Lianyungang network, 2022). However, marine fisheries' rapid development has brought on severe marine ecological problems. The frequency of marine disasters such as marine garbage, red tide and storm surge increases yearly. Some scientific research shows that Enteromorpha prolifera originated in the shoal of Northern Jiangsu, which drifted to the Shandong coast from May to July (Huo et al., 2013; Liu et al., 2013a, 2016). Hence, in the context of ecological protection, it is significant to explore the governing and driving factors of spatiotemporal dynamic changes in mariculture area and analyze the correlation between mariculture and Enteromorpha prolifera outbreaking. All of these can promote the development of mariculture industry and marine environmental protection in Northern Jiangsu.

Based on Landsat images, different classification methods are used to extract the mariculture areas in Haizhou Bay and its adjacent waters in 2013. The extraction method of mariculture areas most suitable for the study area, the object-oriented classification method, is determined. Therefore, this study adopts the object-oriented classification to extract the mariculture areas from 2001 to 2020. The spatiotemporal dynamics of aquaculture areas from 2001 to 2020 are studied by landscape pattern metrics. The driving factors, including nature, society and economy, about spatiotemporal dynamics in mariculture areas are discussed by principal component analysis. Then, we analyze the correlation between mariculture and Enteromorpha prolifera outbreaking. This research result can provide scientific references for the sustainable development of mariculture in Haizhou Bay and its adjacent waters, and impart theoretical support for Enteromorpha prolifera disaster prediction and marine ecological protection.

2. Material and methods

2.1. Study area

Haizhou Bay is located in the northeast of Lianyungang, Jiangsu Province, and the south of Shandong Province (Fig. 1). It is a semi-opened bay of the south Yellow Sea. The water area and coastline length are about 876.3 km^2 and 170 km, respectively. It has a monsoon climate of medium latitudes with sufficient light and high rainfall. The water quality in the bay is fertile, and there are many types of sediment, such as sandy, bedrock, and muddy (Cheng et al., 2009; Zheng et al., 2021). All of these provide a suitable growth environment for raft-aquaculture. The study area is Haizhou Bay and its adjacent waters in the south of Haizhou Bay.

2.2. Data source

Table 1 gives the data requirements of the study, including remote sensing images, driving force analysis data and laver cultivation area data. All of the data were downloaded from the website or provided by other institutions.

In this study, the Landsat image data were downloaded from the United States Geological Survey (USGS). The mariculture in Haizhou Bay is mainly raft-aquaculture, and most of the cultivated crops are laver. The cultivation time is roughly from September of each year to April of the coming year. This study selects 6 Landsat images from November to December in 2001, 2005, 2010, 2013, 2016, and 2020. The data used in 2001, 2005, and 2010 were Landsat 5 TM images with a spatial resolution of 30 m. Landsat 8 OLI images in 2013, 2016, and 2020 were used, including multispectral and panchromatic bands, with spatial resolutions of 30 m and 15 m, respectively. The specific satellite remote sensing data obtained are shown in Table 2. For the Landsat 5 TM image of 2001, 2005, and 2010, the multispectral bands were first calibrated using the Radiometric Calibration tool in ENVI 5.3. Then, the FLAASH Atmospheric Correction tool was used to eliminate the errors caused by atmospheric scattering, absorption, and reflection. The required multispectral image was obtained. For the Landsat 8 OLI image of 2013, 2016, and 2020, radiation calibration and atmospheric correction were also carried out for multispectral bands, and radiometric calibration was performed on the panchromatic band. The Gram-Schmidt Pan Sharpening tool in ENVI 5.3 was used to fuse the multispectral band and the panchromatic band processed in the previous step. The required 15m high-resolution multispectral image was obtained (Zhang et al., 2018b). According to the scope of the study area, the preprocessed image was cropped to acquire the final experimental data.

2.3. Data type and source in this study

This paper analyzes the natural and socio-economic factors to explore the driving force for spatiotemporal dynamic change in the mariculture area. The natural factors include sea surface temperature (SST), wind speed, and the affected area of agriculture, forestry, animal husbandry, and fishery. The data of the affected area were selected from Lianyungang Statistical Yearbook. SST and wind speed were downloaded from Observation data in Chinese oceanic stations of the National Marine Data Center (The National Marine Data Center, 2022). The daily scale data of Lianyungang station from 2000 to 2020 were used to calculate the annual mean SST and wind speed. The socio-economic factors, 13 indicators, such as urbanization level, regional GDP, population, project investment in agriculture, forestry, animal husbandry, and fishery, were selected from Jiangsu statistical yearbook and Lianyungang statistical yearbook.

The experimental flow chart is shown in Fig. 2. The flow chart about the raft-aquaculture area extraction and accuracy evaluation by multiple classification methods is shown in Fig. 2a. Firstly, the raft-aquaculture areas in Haizhou Bay and its adjacent waters in 2013 were extracted

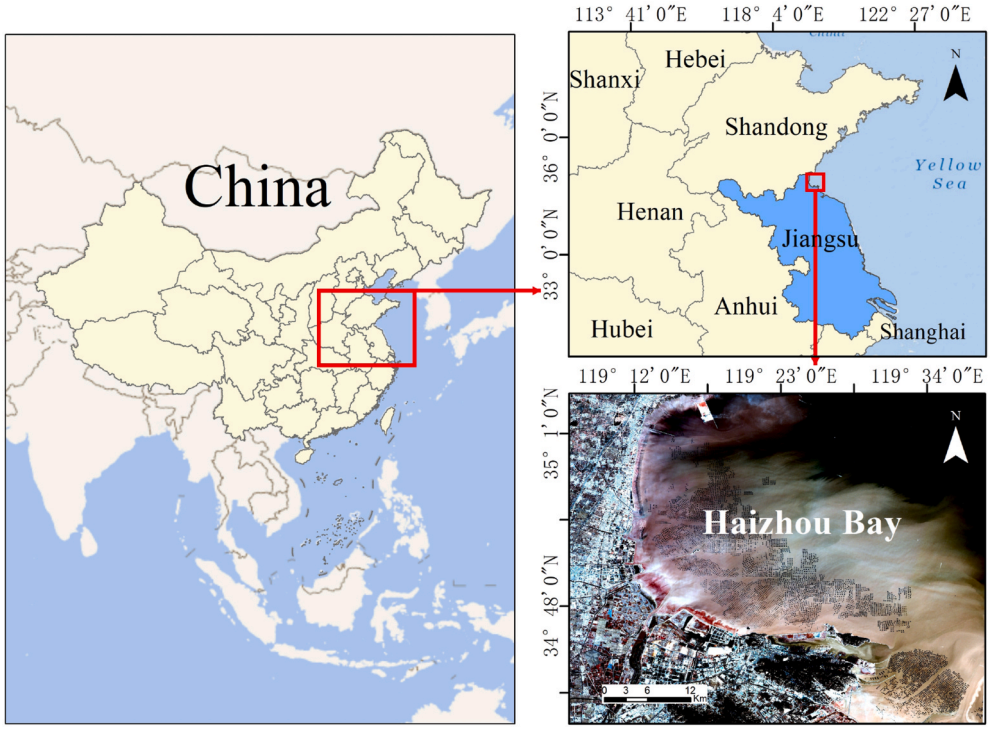

Fig. 1. Marine aquaculture area of Haizhou Bay in Jiangsu Province, China.

Table 1
Data type and source in this study.

Date Types		Names	Time	Source
Remoting Sensing Image		Landsat5 TM Landsat8 OLI	2001,2005,2010. 2013,2016,2020.	USGS (https://glovis.usgs.gov/)
Driving force analysis data	Natural factors	Sea Surface Temperature Wind Speed Surface Salinity	2001–2020	National Marine Data Center (http://mds.nmdis.org.cn/)
		Affected Areas of agriculture, forestry, animal husbandry, and fishery Fertilizer Application Rate		Lianyungang Statistical Yearbook (http://tjj.lyg.gov.cn/tjxxw/)
		Sunshine Duration		Daily Dataset of Surface Climatic Data in China (V3.0)
	Socio-economic factors	Urbanization Level Investment in Lianyungang's agriculture, forestry, animal husbandry, and fishery Total Output Value of agriculture, forestry, animal husbandry, and fishery Average Wage of Employees in agriculture, forestry, animal husbandry, and fishery Power Consumption of agriculture, forestry, animal husbandry, fishery, and water conservancy Affected Areas of agriculture, forestry, animal husbandry, and fishery Regional GDP The proportion of Employees in Primary Industry The proportion of Employees in the Secondary Industry The proportion of Employees in the Tertiary Industry Population Density Population Total Water Resources	2001,2005,2010, 2013,2016,2020.	Jiangsu Statistical Yearbook (https://www.cnki.net); Lianyungang Statistical Yearbook (http://tjj.lyg.gov.cn/tjxxw/)
Laver cultivation area in Jiangsu Province			2004–2005, 2007,2011, 2014–2020.	Jiangsu Statistical Yearbook (https://www.cnki.net)

by object-oriented classification, supervised classification, and band analysis extraction method based on Landsat image. Then, the confusion matrix was calculated by comparing the different extraction results with the results of artificial vectorization. Various indicators were used to verify the classification accuracy of different methods. Fig. 2b shows the extraction and subsequent analysis of the raft-aquaculture area from 2001 to 2020. Firstly, the raft-aquaculture areas in 2001, 2005, 2010, 2013, 2016, and 2020 were classified by object-oriented classification. Then, we conducted the landscape pattern evolution analysis, driving force analysis, and correlation analysis in the follow-up research.

Table 2
Detailed information of satellite remote sensing images.

Image	Imaging Time	Spatial Resolution	Coordinate System	Number of Scenes
Landsat 5 TM	20011130	30 m	WGS_1984_UTM_Zone_50N	1
	20051125	30 m	WGS_1984_UTM_Zone_50N	1
	20101209	30 m	WGS_1984_UTM_Zone_50N	1
Landsat 8 OLI_TIRS	20131201	15 m	WGS_1984_UTM_Zone_50N	1
	20161209	15 m	WGS_1984_UTM_Zone_50N	1
	20201204	15 m	WGS_1984_UTM_Zone_50N	1

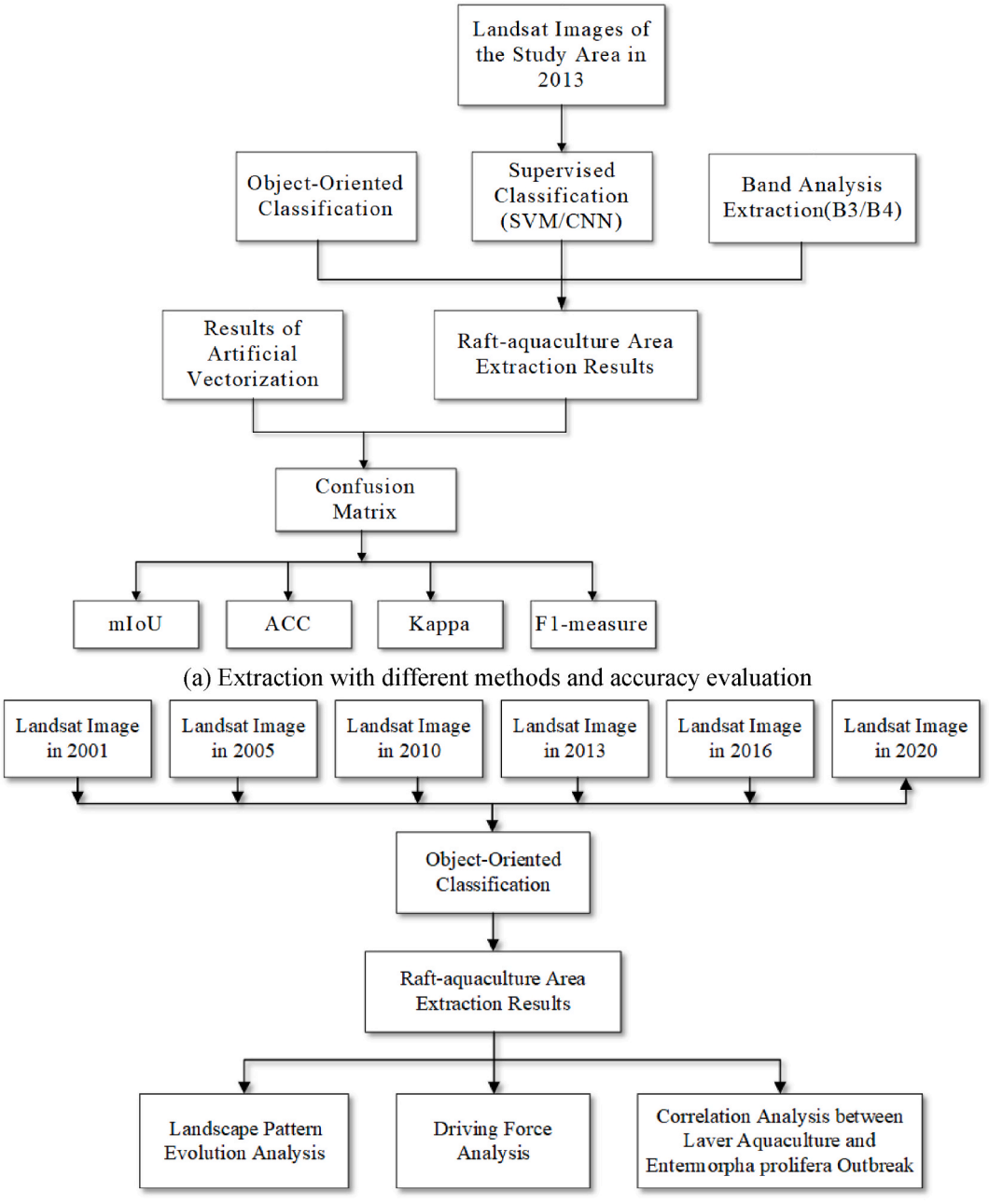

Fig. 2. The experimental flow chart.

2.4. Image classification method

2.4.1. Object-oriented classification

The object-based Image Classification (OBIC) method does not take pixels but the objects generated by image segmentation as the primary classification unit (Li et al., 2020; Luo et al., 2021). This classification method classifies different objects in high-resolution remote sensing images based on spectral features, texture features, geometric shapes, and other information of the images, with high classification accuracy (Huang et al., 2021). Image segmentation is required before object-based image classification. Multi-scale segmentation is a standard segmentation method in object-oriented image interpretation. Considering that surface information has different manifestations at different scales in an image, segmentation is carried out according to different scales of ground objects (Sun et al., 2013; Zhang et al., 2021). The multi-scale segmentation algorithm is based on region-merging technology, starting from merging any pixel until forming an object (image region). In this study, eCognition 9.0.1 is used to classify remote sensing images by object-oriented classification method.

2.4.2. Supervised classification

Supervised classification, also known as training classification, is a process whereby a user identifies pixels of other unknown categories by using pixels of the confirmed category (Zhao, 2003; Xiao et al., 2020). Before classification, positions and sample types of several sample regions are manually selected for the image. Then different classifiers or algorithms are selected to classify other regions into different samples (Li et al., 2017). Supervised classification can be divided into three steps: selecting training samples, extracting statistical information, and choosing the appropriate classification algorithm. In this study, the software ENVI 5.3 was used to realize the supervised classification of remote sensing images. We selected two kinds of classifiers: Convolutional Neural Network (CNN) Classification and Support Vector Machines (SVM) Classification.

2.4.3. Band analysis extraction method

Landsat images in the study area are analyzed. It was found that the brightness of the aquaculture area is lower, and the DN value is smaller, while the brightness of pure water is higher and the DN value is slightly larger. Affected by the spatial distribution pattern of suspended sediment on the nearshore, DN values of pure water bodies and aquaculture raft racks at different locations significantly differ in B2 and B3 bands. In this study, Liu (2013b) research method is referenced to design the image classification.

Each pixel in the study area was statistically analyzed by the neighborhood analysis tool in ArcGIS 10.7. The mean value of all pixels in a rectangular window was taken with the pixel as the center and the side length of 105m. Then, subtracting the newly generated image from the original image of the study band (B2, B3), the result was multiplied by ten thousand and rounded. The positive value represents the water body in the obtained image, and the negative value represents the mariculture region.

2.5. Accuracy evaluation metrics

Confusion Matrix is a standard method for accuracy evaluation. Assuming that the remote sensing images are divided into two categories, the main form of confusion matrix is shown in Table 3. Where TP, FP, TN, and FN represent the number of true positives, false positives, true negatives, and false negatives, respectively.

Table 3
Confusion matrix.

		Predict	
		Positive	Negative
True	Positive	TP	FN
	Negative	FP	TN

In the experiment, mIoU, ACC, Kappa, and F1-measure are used to verify the accuracy of different classification methods. The four parameters are defined as follows:

$$mIoU = \frac{TP}{(FP + FN + TP)} \tag{1}$$

$$ACC = \frac{TP + TN}{TP + TN + FP + FN} \tag{2}$$

$$F1 - measure = \frac{2 \times precision \times recall}{precision + recall} \tag{3}$$

$$Precision = \frac{TP}{TP + FP};\ Recall = \frac{TP}{TP + FN} \tag{4}$$

$$Kappa = \frac{N\sum_{i=1}^{n} x_{ii} - \sum_{i=1}^{n}(x_{i+}x_{+i})}{N^2 - \sum_{i=1}^{n}(x_{i+}x_{+i})} \tag{5}$$

The Kappa coefficient assumes that remote sensing images are divided into N categories, and N is the total sample number of ground truth. We consider the classification results of raw remote sensing images to be ground truth. x_{ii} is the number of correctly classified pixels. x_{i+} is the sum of the $i-th$ row, and x_{+i} is the sum of the $i-th$ column about the confusion matrix.

Taking the Landsat8 OLI remote sensing image of Haizhou Bay in 2013 as the base map, the polygon shapefile was created using arcgis10.7, on which the visual interpretation of the raft-aquaculture area was performed to obtain the artificial vectorized results. In order to verify the classification results, artificial vectorized data of raft-aquaculture areas are used as true values to calculate the confusion matrix with different classification results. The aquaculture area is a positive sample in the actual image, and the sea is a negative sample. In the experiment, the four parameters, mIoU, ACC, Kappa, and F1-Measure, are used to verify the accuracy of different classification methods.

2.6. Landscape pattern indices

The landscape pattern indices are a typical method to quantitatively describe landscape patterns and measure landscape spatial attributes. It can explain the landscape distribution level of a region and reflect the changes in landscape structural characteristics and spatial patterns (Nadoushan and Alebrahim, 2017; Song et al., 2017). The landscape pattern indices incorporate patch level index, patch class index, and landscape-level index. The patch level index represents the structural characteristics of individual patches in the landscape. Patch class index can express the structural characteristics of different patch types in the landscape. The landscape-level index can reflect the structural characteristics of the entire landscape.

In this study, the software Fragstats 4.2 is adopted to calculate the landscape pattern indices during the six years from 2001 to 2020. According to the status quo and spatial structure characteristics of the study area, six indices, including Total Area (TA), Number of Patches (NP), Patch Density (PD), Landscape Shape Index (LSI), Splitting Index (SPLIT) and Aggregation Index (AI), were selected to analyze the landscape pattern evolution of raft-aquaculture area in Haizhou Bay (Table 4).

2.7. Principal component analysis

Principal Component Analysis (PCA) is a relatively common method

Table 4
The description of landscape pattern indices.

	Name	Description
TA	Total Area	It is the sum of all patch areas in a patch type, which is the basic area indicator.
NP	Number of Patches	It is the total number of patches of a certain patch type, which has a good positive correlation with landscape fragmentation.
LSI	Landscape Shape Index	It reflects the changing rule of patch shape in the landscape. The larger the value, the more irregular the patch's shape in the landscape will increase.
PD	Patch Density	The number of certain patches per 100 ha.
SPILT	Splitting Index	It indicates the overall fragmentation degree of the landscape. The higher the value, the greater the impact of human activities on the landscape.
AI	Aggregation Index	The aggregation degree of a patch type in the landscape. The larger the value, the more compact the aggregation degree.

of multivariate analysis. The data are first transformed into a new coordinate system using a linear transformation; then dimensionality reduction is used so that the first major variance of any data projection is in the first coordinate (called the first principal component), and the second major variance is in the second coordinate (the second principal component) (Liu et al., 2020). Dimensionality reduction can reduce the dataset's dimensionality and maintain the dataset's characteristics that contribute most to the variance. The goal is to extract the most important information from the data and compress the size of the dataset by keeping the important information.

Thirteen socio-economic indicators were selected by reviewing the Lianyungang City Statistical Yearbook from 2001 to 2020. The factor variables were constructed by PCA using IBM SPSS Statistics 26 software. The specific steps are as follows.

Firstly, create a sample matrix of socio-economic indicators and standardize the indicator data in the sample matrix to obtain a standardized data matrix. Secondly, create a covariance matrix based on the standardized data matrix. Thirdly, calculate the eigenvalues, contribution rates and cumulative contribution rates based on the covariance matrix, and rank the corresponding eigenvalues according to their sizes, with the largest eigenvalue being the first principal component, the second largest eigenvalue being the second principal component, and so on, from which the first three principal components are extracted in this paper. The cumulative variance contribution rate has reached 85%, which can explain the change pattern of the Haizhou Bay aquaculture area. Fourthly, the principal component loadings matrix and principal component loadings rotation matrix are calculated to determine the key indicators. Finally, the scores of each principal component are calculated.

3. Results

3.1. Experiment and accuracy evaluation

In order to find the most suitable method for extracting aquaculture

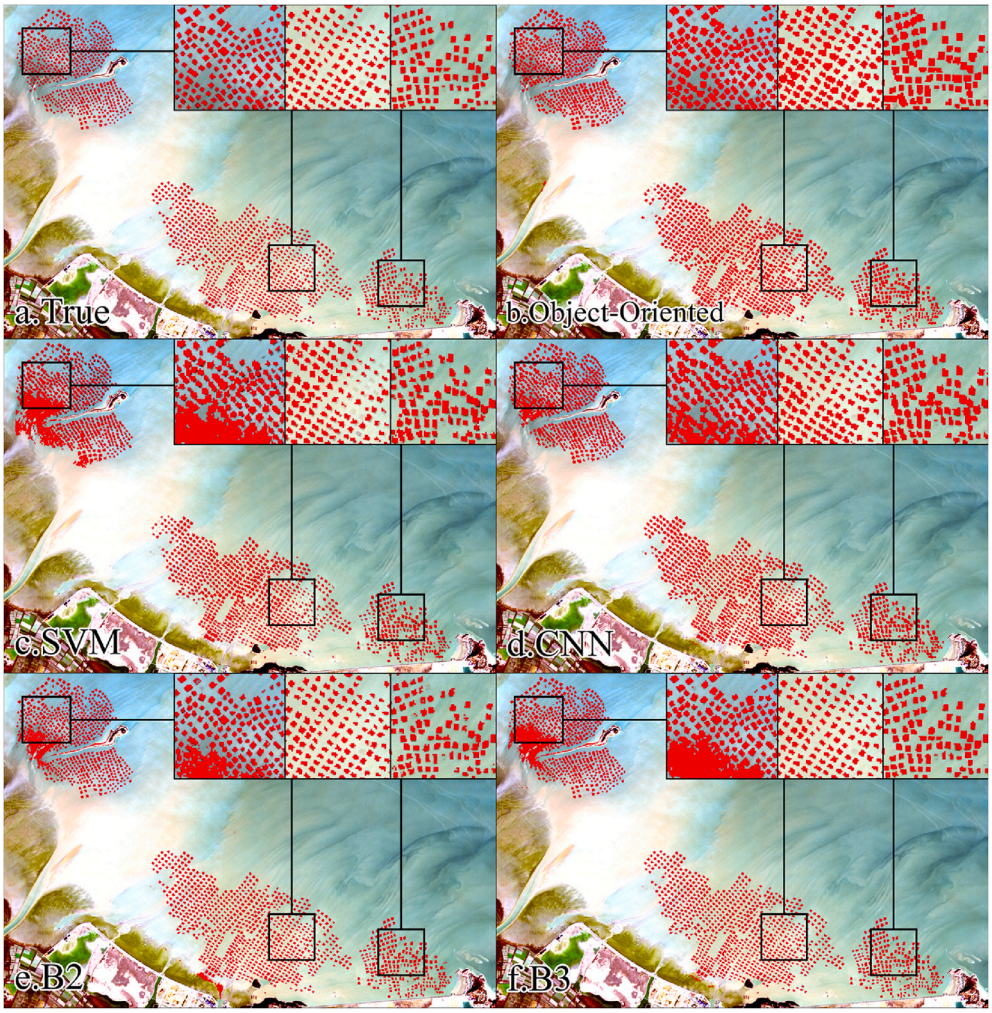

Fig. 3. Extraction results of aquaculture areas by different classification methods. (a)True value, (b) Object-Oriented classification, (c)SVM, (d)CNN, (e)B2, (f)B3.

areas, methods, including CNN, SVM, object-oriented classification and feature variable extraction, were used to extract raft-aquaculture areas in the images of 2013. Corresponding classification results were obtained (Fig. 3). Fig. 3a shows the true results of aquaculture areas obtained by artificial vectorization. Fig. 3b–f shows the results extracted by the above classification method. From the comparative analysis of Fig. 3b–f and Fig. 3a, it can be seen that the classification effect of Fig. 3b is the most similar to that of Fig. 3a on the whole. The misclassification and omission are also relatively less. In Fig. 3c–f, the misclassification phenomenon is relatively evident, concentrated in the northwest of the experimental area. The models mostly misidentify the aquaculture raft racks as the sea. At the same time, due to the color difference of the sea, many shallow raft racks seen by naked eyes in the image cannot be correctly identified by the model, resulting in the omission of classification.

Four parameters, including mIoU, ACC, Kappa, and F1-Measure, which is used to verify the accuracy of different classification methods are shown in Table 5. It shows that the mIoU, ACC, Kappa, and F1-measure of object-oriented classification method are the highest among the five classification methods. It can be seen that this method has the highest accuracy, which is suitable for the extraction of mariculture rafts in Haizhou Bay. Hence, in this study, we select the object-oriented classification method to extract the raft-aquaculture area in Haizhou Bay and its adjacent waters from 2001 to 2020.

3.2. Spatial information extraction and landscape pattern evolution analysis

Fig. 4 shows the extraction results about aquaculture raft racks in Haizhou Bay and its adjacent areas in 2001, 2003, 2010, 2013, 2016, and 2020 through object-oriented classification method. It can be roughly seen from Fig. 4a–f that the number of aquaculture raft racks increased from 2001 to 2020. With the increasing amount of aquaculture raft racks, the raft-aquaculture area is also expanding from the coastal waters of the mainland to the ocean's interior. The expansion speed is very rapid.

The calculation results of landscape pattern indices, including Total Area (TA), Number of Patches (NP), Patch Density (PD), Aggregation Index (AI), Splitting Index (SPLIT) and Landscape Shape Index (LSI), are illustrated in Table 6. It is shown from Fig. 5 that the TA increased quickly from 2001 to 2016 but then decreased slowly from 2016 to 2020. From 2001 to 2010, TA increased gradually from 141.9 ha to 2212.3 ha, with an annual increase of 230 ha. From 2010 to 2016, TA increased rapidly from 2212.3 ha to 15766.4 ha, with an average annual increase of 2259.1 ha. From 2016 to 2020, it fell slightly from 15766.4 ha to 13672.1 ha.

NP shows an increasing trend (Fig. 5b), with the growth rate from slow to fast. It increased from 119 to 6387 from 2001 to 2020, with 53.7 times and an annual increase of 330 PD is the number of patches per 100 ha. It shows the characteristics of fluctuation from increase to decrease and then to increase. From 83.8 patches per 100 ha in 2001 to 46.7 patches per 100 ha in 2020, the overall reduction is 37 patches per 100 ha. AI decreased gradually and then increased, and the overall degree of aggregation is high. From 2001 to 2020, LSI gradually increased from 12.2 to 95.4, indicating that the patch shape irregularity also increased, and the patch shape became more complex and irregular. SPLIT shows the fluctuation characteristics of first increasing, then decreasing, and finally increasing. Overall, SPLIT increased from 67.6 to 1177.1. The overall landscape fragmentation is severe and scattered, the aquaculture area gradually expands to the interior of the sea, and its spatial distribution is growing complicated, demonstrating that the interference intensity of human activities with the mariculture gradually increases.

In general, NP, PD, LSI, and SPLIT are increasing, indicating that aquaculture zones' heterogeneity and fragmentation degree in Haizhou Bay and its adjacent waters are increasing. Patch shapes of aquaculture raft racks are becoming more complex. The aquaculture raft racks in Haizhou Bay are expanding in spatial distribution, and the center of mass about the aquaculture area shifts from southwest to northeast. The aquaculture industry lacks planning, and tends to develop in disorder. With the rapid development of the mariculture industry in recent years, the development and utilization of ocean have increased. Therefore, the human management of the landscape should be gradually strengthened in Haizhou Bay, the mariculture structure should continue to improve, and the scale and intensification degree of the breeding industry should also be gradually improved.

Table 5
Accuracy evaluation of classification results in 2013.

Method		mIoU	ACC	Kappa	F1
Object-oriented Classification		0.82	0.90	0.79	0.80
Supervised Classification	CNN	0.71	0.58	0.61	0.62
	SVM	0.73	0.67	0.64	0.66
Band Analysis Classification	B2	0.74	0.56	0.67	0.68
	B3	0.76	0.60	0.69	0.70

4. Discussion

4.1. Driving force analysis of raft-aquaculture areas changes

4.1.1. Natural factors

From 2001 to 2020, the mariculture industry in Haizhou Bay and its adjacent waters developed rapidly. The patch area increased from 141.93 ha in 2000 to 13,672.08 ha in 2020, which is closely related to natural factors. According to the statistical data, laver can grow at an optimum temperature of 0.5–18 °C. Laver leaves will quickly rot when the seawater temperature exceeds 20 °C (Kim, 2013). The average SST from 2000 to 2020 is maintained at 15–17 °C, always providing a suitable temperature for laver aquaculture. Meantime, the optimum salinity for the growth of laver seedlings is in the range of 20.3–40.6, within which the higher the salinity, the higher the percentage of developing into normal seedlings (Yan and Wang, 1993). From 2001 to 2020, the surface salinity of seawater in the Haizhou Bay region is maintained between 25 and 29, which is moderate salinity and can maintain the suitable growth of laver. It's well known that nutrients (N and P) and sunlight are key factors for biomass growth. According to statistics, the suitable daily sunshine duration for the growth of laver is 7–8 h, and the sunshine duration from 2001 to 2020 is between 1950 h and 2300 h, which can promote the healthy growth of laver. Fertilization methods for laver mainly include the spraying method and soaking method, etc. The amount of fertilizer application for agricultural use in Lianyungang City showed an increase from 2001 to 2014 and a slight decrease from 2015 to 2020. This is related to the Ministry of Agriculture issued "Zero Growth Action Plan for Fertilizer Use by 2020″ in 2015, which requires the adjustment of fertilizer structure, the replacement of chemical fertilizers with organic fertilizers, and the reduction of precise fertilizer application (The Ministry of Agriculture of the People's Republic of China, 2020). Proper fertilization can promote the photosynthesis of laver and improve the yield.

The annual average wind speed and the affected area of agriculture, forestry, animal husbandry, and fishery are statistically analyzed. As shown in Fig. 6a, the annual average wind speed fluctuates between 4.5 m/s and 5.5 m/s, and tends to decrease year by year. When the wind speed is too high, the raft racks of laver aquaculture will be overturned and pulled up. When the wind speed decreases, the damage degree of raft racks will be reduced, promoting the cultivation of the laver to a certain extent.

The affected area of agriculture, forestry, animal husbandry, and fishery in the vicinity of the study area shows an overall downward trend from 2001 to 2020 (Fig. 6b). From 2001 to 2003, natural disasters frequently occurred in the study area, with an average annual affected area of more than 2,200,000 ha (Table 7). The affected areas exceeded

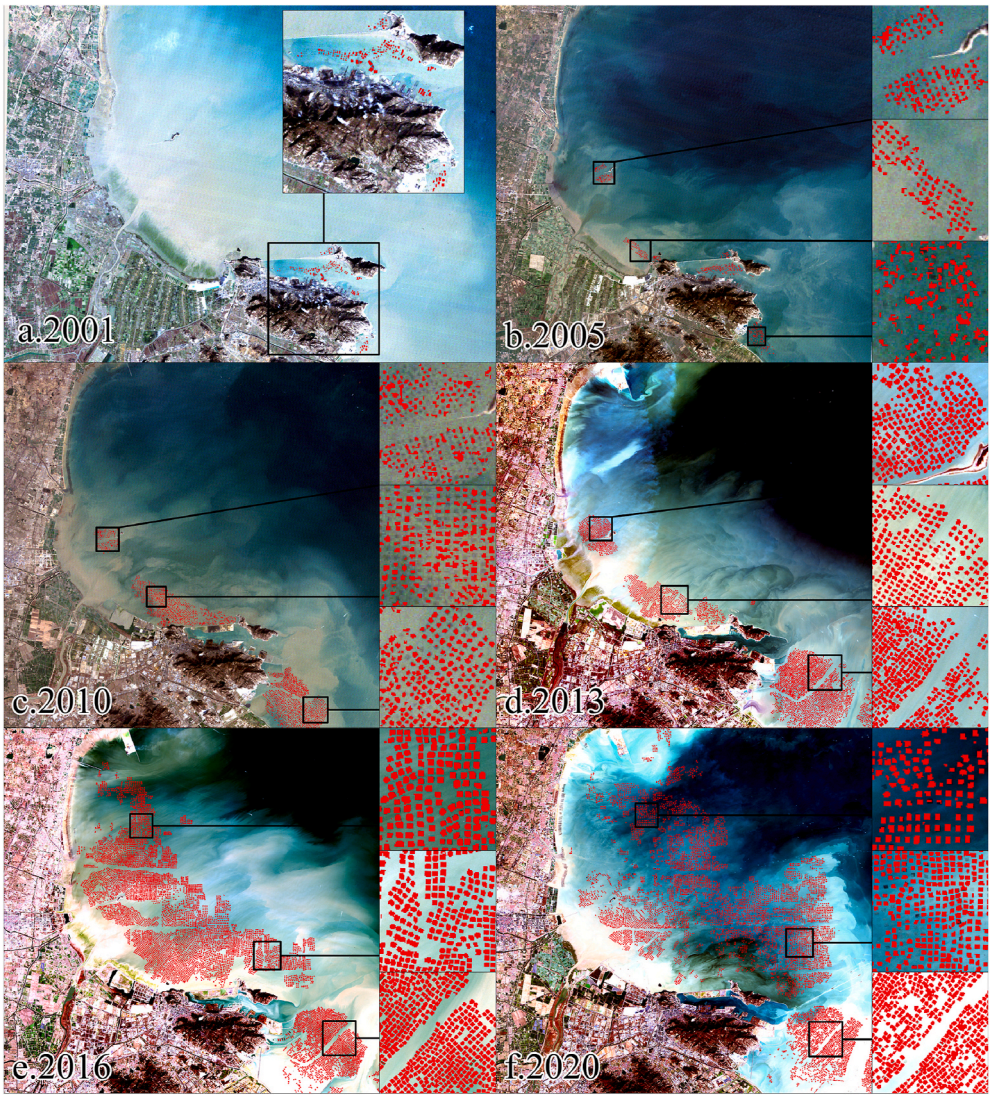

Fig. 4. The extraction results of mariculture areas from 2001 to 2020 (a) 2005, (c) 2010, (d) 2013, (e) 2016, (f) 2020.

Table 6
Calculation results of different landscape metrics.

Year	TA	NP	PD	LSI	SPLIT	AI
2001	141.9	119	83.8	12.2	67.6	70.9
2005	457.8	499	109.0	27.6	240.3	62.2
2010	2212.3	1868	84.44	53.6	950.1	66.2
2013	5595.1	1958	34.99	67.6	23.9	73.2
2016	15766.4	4929	31.26	95.4	161.6	77.4
2020	13672.1	6387	46.72	95.9	1177.1	75.6

1,000,000 ha in 2005, 2006, 2007, 2010, 2011, and 2012. Natural disasters not only have a great negative effect on the stability of the ecosystem in the study area but also seriously affect regional industrial and agricultural development and fishery production. From 2013 to 2020, the affected area decreased from 487,360 ha to 131,000 ha. The reduction of natural disasters stabilized the environment of laver cultivation, promoting the development of cultivation industry. It is also one of the main causes why the patch area of aquaculture area has increased rapidly since 2013.

4.1.2. Socio-economic factors

The status quo of Haizhou Bay and its adjacent waters is discussed, the research results of prominent scholars are used for reference, and the availability of data is considered (Cui et al., 2019c; Luo et al., 2019). The principal component analysis (PCA) is used to analyze the correlation between each index and landscape pattern evolution is analyzed, and the statistical data used in PCA are shown in Table 8.

The eigenvalue and Principal component contribution rate are shown in Table 9. It shows that cumulative contribution rate of the first principal component and the second principal component has reached 86.99%, and the eigenvalues are greater than 1, which can meet the analysis requirements. Loads of the first two principal components on each variable after rotation are shown in Table 10. It can be seen that the first principal component has a heavy load on investment and average employee wage of the primary industry, the city's GDP, and other indicators, which can be summarized as a comprehensive factor of the economy. The second principal component has a heavy load on population, people density, the proportion of employees in each industry, and other indicators, summarized as social and demographic factors. Therefore, the driving factors of landscape pattern evolution in the study area can be roughly divided into economic and social demographic factors.

In terms of economic factors, the GDP of Lianyungang City increased from 24.907 billion Chinese Yuan (CNY) to 327.707 billion Chinese Yuan (CNY) from 2001 to 2020, an increase of more than 13 times. Among them, the total output value of agriculture, forestry, animal

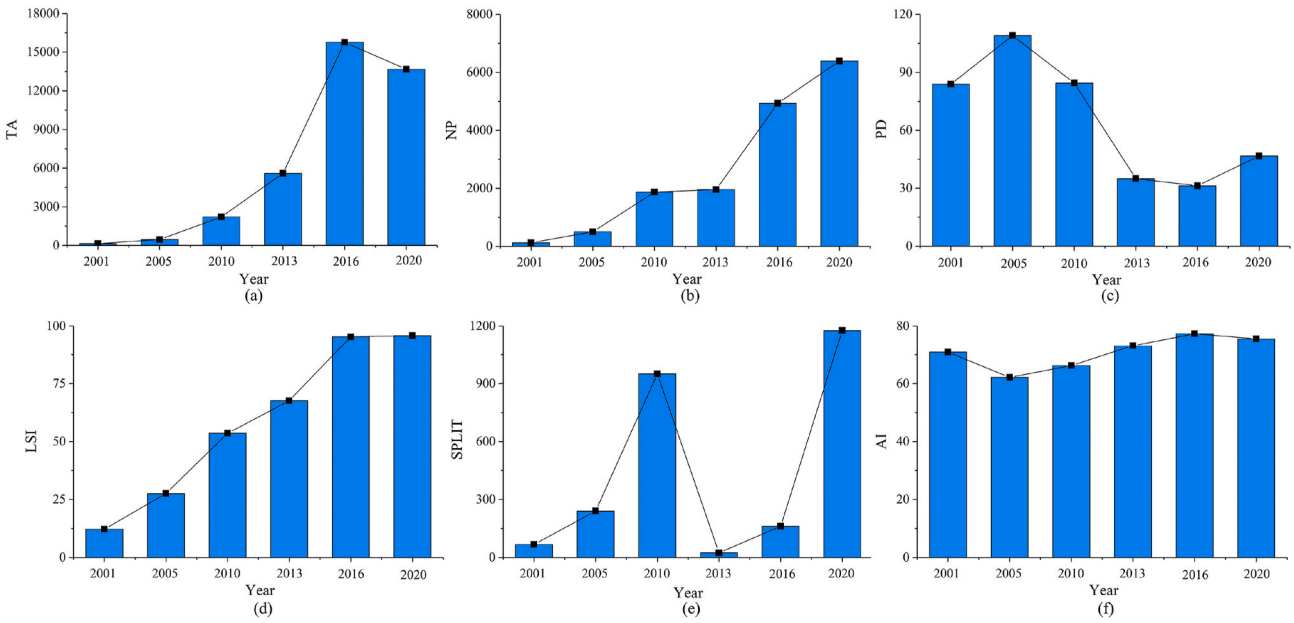

Fig. 5. The changes in landscape metrics of Haizhou Bay aquaculture raft racks from 2000 to 2020 (a) TA (b) NP (c) PD (d) LSI (e) SPLIT (f) AI.

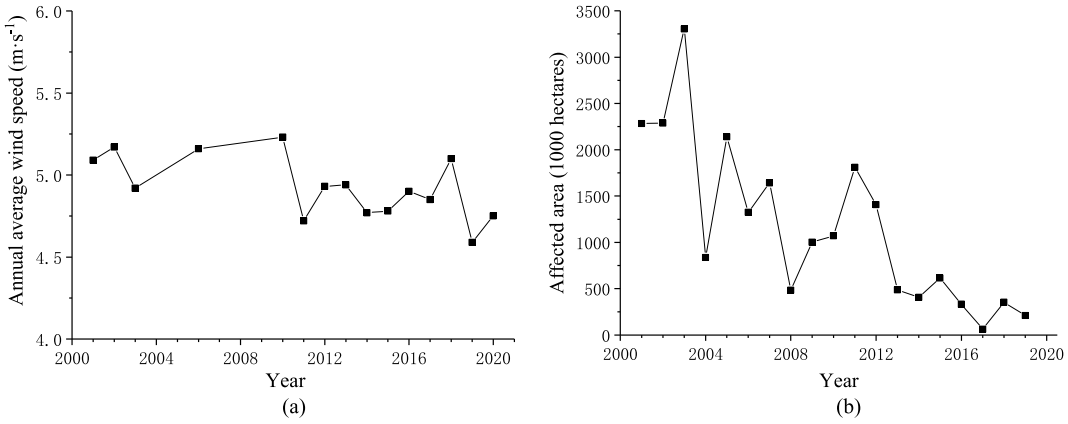

Fig. 6. Changes in the annual average wind speed (a) and the affected area of agriculture, forestry, animal husbandry, and fishery (b) in the study area from 2000 to 2020.

husbandry, and fishery increased from 14.905 billion Chinese Yuan (CNY) to 70.248 billion Chinese Yuan (CNY), which increased by 4.7 times. The average wage of employees engaged in agriculture, forestry, animal husbandry, and fishery in cities has also increased from 4447 Chinese Yuan (CNY) to 62917 Chinese Yuan (CNY). The level of urbanization is constantly improving. Lianyungang has an excellent geographical location, convenient transportation, and shipping conditions. Integrating the advantages of geography, location, and policy, it has become another free trade pilot zone in China, which currently is provided with the conditions for deep opening up to the outside world. In recent years, the government increased investment in fishery-related projects, and the import and export trade in Lianyungang is thriving. In the meantime, the people's living standards improve constantly. Hence, the demand for fishery products has risen rapidly. The development of mariculture in Lianyungang has been promoted to a certain extent. It is one of the fundamental reasons for the increasing mariculture area in Haizhou Bay and its adjacent waters from 2001 to 2020.

From the perspective of social and demographic factors, from 2001 to 2020, the total population of Lianyungang City increased from 4.5699 million to 4.601 million. Moreover, the population density also increased gradually. The increase in population promotes the social demand for natural resources. In recent years, the international market demand for laver products has been increasing, and the domestic market demand for seaweed products is also growing at a rate of 10–15% per year. Therefore, in addition to meeting the needs of the people of Lianyungang, in order to meet the needs of the international and domestic markets, it requires more agricultural and fishery products to meet the needs of people's survival. Technologies related to fisheries, such as mariculture and mechanized fisheries production, tend to mature. Human and material resources have been poured into the industry. Mariculture is gradually developing towards standardization, mechanization, and internationalization. The crop yield significantly increases. The seafood produced in this region has great core competitiveness in the market. At the same time, the industrial transformation of Lianyungang City has led to a continuous reduction in the proportion of employees in the primary industry. With the continuous adjustment of industrial and employment structure, the employees continuously transfer from the primary industry to the secondary and tertiary industries (Li, 2016). In recent years, the mechanized production system of aquaculture has been established. The aquaculture industry is transformed and upgraded to green and efficient. The effect of the labor-intensive model on mariculture is gradually decreasing.

Table 7
Statistical data of annual mean SST, wind speed, affected area, annual average surface salinity, fertilizer application rate and annual sunshine duration in Haizhou Bay from 2001 to 2020.

	Annual mean SST (°C)	Annual average wind speed (m/s)	The affected area (One thousand ha)	Annual average surface salinity (g/kg water)	Fertilizer application rate (One million tons)	Annual sunshine duration (h)
2001	15.66	5.09	2283.24	28.64	31.58-	2167.42
2002	–	5.17	2288.46	–	–	2124.28
2003	16.88	4.92	3305.00	27.89	–	2209.92
2004	–	–	836.58	28.35	–	1950.50
2005	16.21	–	2139.50	27.69	32.06	2286.89
2006	–	5.16	1324.07	28.13	–	2231.38
2007	–	–	1642.00	27.26	32.20	2001.21
2008	–	–	483.70	26.25	–	2018.30
2009	–	–	1001.63	28.43	34.93	1992.12
2010	16.75	5.23	1070.93	–	33.82	1992.84
2011	–	4.72	1810.60	28.69	33.73	2125.29
2012	15.31	4.93	1406.45	27.00	33.77	2055.37
2013	14.60	4.94	487.36	27.89	34.23	2050.07
2014	15.11	4.77	407.69	–	34.58	2240.92
2015	–	4.78	615.46	28.16	34.55	2055.05
2016	–	4.90	332.10	27.41	34.57	2012.42
2017	16.37	4.85	62.29	26.54	33.26	2059.46
2018	16.54	5.10	353.73	25.85	32.43	2321.15
2019	16.24	4.59	210.81	27.29	32.02	2197.75
2020	16.15	4.75	131.00	26.40	31.29	2056.46

Table 8
Statistical data used in PCA.

	2001	2005	2010	2013	2016	2020
Urbanization Level (%)	28.02	37.18	51.75	54.82	57.80	61.52
Investment in agriculture, forestry, animal husbandry, and fishery (Ten thousand CNY)	4561	42563	98416	176104	475414	511454
The total output value of agriculture, forestry, animal husbandry, and fishery (One hundred million CNY)	149.05	174.02	322.80	474.24	589.42	702.48
Average Wage of Employees in agriculture, forestry, animal husbandry, and fishery (CNY)	4447	6725	19296	30147	46697	62917
Power Consumption of agriculture, forestry, animal husbandry, fishery, and water conservancy (one Million kilowatt-hours)	43.53	29.12	28.36	43.40	61.87	53.76
Affected Areas of agriculture, forestry, animal husbandry, and fishery (one thousand ha)	2283.24	2139.50	1070.93	487.36	332.10	131.00
Regional GDP (One hundred million CNY)	249.07	455.97	1201.79	1829.04	2536.49	3277.07
The proportion of Employees in Primary Industry (%)	58.10	43.80	30.50	32.70	31.40	27.70
The proportion of Employees in the Secondary Industry (%)	20.30	26.10	31.70	31.30	32.20	30.60
The proportion of Employees in the Tertiary Industry (%)	21.60	30.10	37.80	36.00	36.40	41.10
Population Density (Person/km^2)	702.20	743.40	759.00	818.50	739.40	749.30
Population (10,000 people)	456.99	454.40	439.71	445.98	453.93	460.10
Total Water Resources (One hundred million m^3)	30.43	53.69	26.21	27.87	20.90	40.70

(Note: The primary industry is agriculture, forestry, animal husbandry, and fishery, the secondary industry is the processing and manufacturing industry, and the tertiary industry is other industries other than the primary and secondary industries. CNY: Chinese Yuan).

Table 9
Eigenvalue and Principal component contribution rate.

Principal component	Eigenvalue	Contribution rate/%	Cumulative contribution rate/%
1	6.864	52.799	52.799
2	4.301	34.187	86.986

Table 10
Rotated component matrix.

Indicators	Principal component 1	Principal component 2
Investment in agriculture, forestry, animal husbandry, and fishery	0.984	0.128
Average Wage of Employees in agriculture, forestry, animal husbandry, and fishery	0.961	0.258
Regional GDP	0.941	0.328
The total output value of agriculture, forestry, animal husbandry, and fishery	0.932	0.343
Power Consumption of agriculture, forestry, animal husbandry, fishery, and water conservancy	0.869	−0.296
Affected Areas of agriculture, forestry, animal husbandry, and fishery	−0.806	−0.541
Urbanization Level	0.746	0.657
Population Density	0.045	0.838
The proportion of Employees in Primary Industry	0.500	0.826
The proportion of Employees in the Secondary Industry	−0.588	−0.794
The proportion of Employees in the Tertiary Industry	0.616	0.765
Population	0.497	−0.751
Total Water Resources	−0.178	−0.130

4.2. Relationship between laver aquaculture and entermorpha prolifera outbreak

Globally, green tides, caused by the explosive proliferation of large-scale marine green algae, have become the universal marine ecological phenomena. As a type of green algae, Enteromorpha prolifera has become one of the significant marine disasters in China in the past decade, resulting in a series of ecological and environmental problems and economic losses (Jiang and Zhao, 2018). The disaster of Enteromorpha prolifera in China is mainly concentrated in the Yellow Sea area. From April to May every year, the green tide drifts northward from the South Yellow Sea under the action of ocean currents and wind, and makes landfall in cities along the coast of Shandong. Green tide accumulates on the coast on a large scale after landing. It not only endangers the ecological environment and people's health but also impacts local

tourism (Zhang et al., 2018a, 2020; Cui et al., 2019b). In 2021, the scale of the Enteromorpha prolifera disaster in the Yellow Sea reached the largest in history. After investigation and verification, it is roughly confirmed that the floating green tide originated from the laver aquaculture area of outer sand in southern Jiangsu province. This is closely related to the local unique marine environment and laver culture methods. Therefore, the correlation between laver aquaculture and Enteromorpha prolifera outbreak should be studied, which is crucial to grasp the outbreak time node and prevent and subsequently control such a disaster.

Many studies have found that the scale of the green tide outbreak in the Yellow Sea is directly related to the initial biomass of green algae. However, the initial biomass of green algae is closely related to the laver cultivation area (Li et al., 2014). Jiangsu shoal mainly adopts semi-floating raft-aquaculture as China's most extensive laver cultivation base. Green algae such as Enteromorpha prolifera, as the attached organisms on the raft racks, appear at the beginning of the annual laver aquaculture. Only a few Enteromorpha prolifera individuals fall off and float in the process of production. In the early stage of laver cultivation, it is not easy to form a large scale of Enteromorpha prolifera. In the latter, in recycling the rope after the laver is harvested, the green tide algae are usually scraped off to reduce the rope's weight. This causes green algae to detach from their attachment and drift into the ocean, which provides the initial biomass for the formation of green tides (Wang et al., 2015).

In recent years, the continuous expansion of laver cultivation area has increased the amount of nutrients entering the ocean and the initial biomass of green tide. Studies have shown that the unique biological characteristics of Enteromorpha prolifera, suitable environment, and climate factors in the northern Jiangsu sea area are the crucial reasons why the disaster of green tide frequently occurs (Quillien et al., 2015; Hao et al., 2021). According to the statistical yearbook of Jiangsu Province (Table 11), the laver cultivation type in Jiangsu province is mainly Porphyra yezoensis. From 2004 to 2020, the laver cultivation area increased from 8466 ha to 46,667 ha. The cultivation area in 2020 was more than 5 times that in 2004. Due to the small cultivation area in the past, the aquaculture was mainly concentrated in the inner sand near the shore. With the increasing aquaculture area in recent years, the aquaculture range extends from inshore inner sand to outer sand, from intertidal zone beach to subtidal zone shallow water area. Nowadays, the aquaculture area of outer sand has exceeded the inner sand. The cultivation area of the laver in outer sand increased significantly in 2007, nearly doubling that in 2005. The biomass of green algae in the raft racks has increased significantly, so the green tide in the Yellow Sea began to break out in 2007. Since 2007, the cultivation area of the laver in Jiangsu Province has continued to rise, which provides sufficient initial biomass for the outbreak of green tide. Therefore, the green tide in the Yellow Sea will arrive as scheduled every year, and the coverage area of Enteromorpha prolifera has an increasing trend year by year. The disease of Porphyra yezoensis in Jiangsu Province was serious from late December to mid-December 2011. The phenomenon of rotten vegetables occurred in a large area, and the proportion of rotten vegetables in the area of laver aquaculture reached about 70%. The area of no harvest exceeded 30% in 2011, and the aquaculture net curtain, raft racks, and other equipment, which had no harvest, were brought ashore in advance (JiangsuLaver Association, 2012). It was observed that in 2012, the occurrence time of the green tide disaster was significantly earlier, and the coverage area of the green tide was correspondingly reduced. It again verifies the correlation between laver aquaculture and the outbreak of green tide.

Table 11
Laver cultivation area in Jiangsu Province from 2001 to 2020.

Year	Cultivation area of laver/ha
2004	8466
2005	10866
2007	21600
2011	21133
2014	39024
2015	29618
2016	41066
2017	47255
2018	43111
2019	41666
2020	46667

5. Conclusion

Based on Landsat remote sensing images, this paper extracts the mariculture area by using object-oriented classification method. The spatio-temporal distribution, area and landscape pattern of mariculture areas in Haizhou Bay from 2001 to 2020 were studied. Meanwhile, the driving forces from natural, social and economic aspects of the mariculture areas evolution were discussed by using PCA and other methods. The correlation between mariculture and Enteromorpha prolifera outbreak was evaluated. The conclusions are as follows:

1. From 2001 to 2020, aquaculture in Haizhou Bay and its adjacent waters changed significantly. The cultivation area showed a trend of increasing first and then slowing down. After reaching its peak in 2016, it decreased. Nevertheless, it shows an overall increasing trend over these years. The aquaculture zone spreads from the coast of Lianyungang city to the ocean's interior.
2. According to the landscape pattern evolution analysis, the NP, PD, LSI, and SPLIT of Haizhou Bay and its adjacent sea waters are increasing yearly. The heterogeneity and fragmentation of aquaculture areas are increasing, and the patch shape is becoming more and more complex. The impact of human beings on the landscape is also gradually strengthening.
3. The increasing of aquaculture area, heterogeneity and fragmentation in Haizhou Bay and its adjacent waters are related to many factors. The main influencing factors are natural factors and socio-economic factors. The factors, including suitable sea temperature, low wind speed, small disaster area of the fishery, high-speed economic development, and social progress, could positively impact the development of marine aquaculture.
4. The outbreak of Enteromorpha prolifera in the Yellow Sea has a specific correlation with laver cultivation in Jiangsu coastal areas. Mariculture can provide the initial biomass source for the formation of green tide. The larger the area of laver cultivation, the larger the scale of the green tide outbreak in the Yellow Sea.
5. In this study, the remote sensing method is used to monitor the mariculture area, which can save manpower and material resources. It provides a scientific reference for marine environment protection, prevention, and control of green tide disasters. At the same time, there are also problems, such as low image spatial resolution, which can be improved in subsequent experiments.

Author statement

Bo Ai: Conceptualization, Methodology, Investigation, Writing-Original Draft, Writing- Review & Editing.

Peipei Wang: Supervision, Investigation, Writing-Original Draft, Writing- Review & Editing.

Zhengyi Yang: Investigation, Writing-Original Draft, Writing- Review & Editing.

Yuxin Tian: Investigation, Writing- Review & Editing.

Dandan Liu: Writing- Review & Editing.

All authors have read and agreed to the published version of the manuscript.

Declaration of competing interest

The authors declare that they have no known competing financial interests or personal relationships that could have appeared to influence the work reported in this paper.

Data availability

The authors do not have permission to share data.

Acknowledgements

This work was supported by the National Natural Science Foundation of China [grant numbers 62071279; 41930535].

References

Agriculture Fisheries Bureau, 1, 2019. Some Opinions on Accelerating the Green Development of Aquaculture. China Fisheries.

Blondeau-Patissier, D., Gower, J.F.R., Dekker, A.G., Phinn, S.R., Brando, V.E., 2014. A review of ocean color remote sensing methods and statistical techniques for the detection, mapping and analysis of phytoplankton blooms in coastal and open oceans. Prog. Oceanogr. 123, 123–144. https://doi.org/10.1016/j.pocean.2013.12.008.

Boyd, C.E., D'Abramo, L.R., Glencross, B.D., Huyben, D.C., Juarez, L.M., Lockwood, G.S., McNevin, A.A., Tacon, A.G.J., Teletchea, F., Tomasso, J.R., Tucker, C.S., Valenti, W. C., 2020. Achieving sustainable aquaculture: historical and current perspectives and future needs and challenges. J. World Aquacult. Soc. 51, 578–633. https://doi.org/10.1111/jwas.12714.

Chen, S., 2021. Spatiotemporal dynamics of mariculture area in Sansha Bay and its driving factors. Chinese Journal of Ecology 40, 1137–1145. https://doi.org/10.13292/j.1000-4890.202104.033.

Chen, X., Chen, J.Z., 2020b. Countermeasures for marine environmental pollution governance: an ecological civilization perspective. J. Coast Res. 106, 355–358. https://doi.org/10.2112/SI106-082.1.

Chen, H., Li, W., Xie, X., 2020. Intelligent image monitoring technology of marine environmental pollution information. J. Coast Res. 112, 1–4. https://doi.org/10.2112/JCR-SI112-001.1.

Cheng, J., Zhang, Y., Zhang, D., Liu, J., Chen, S., 2009. Analysis of ecological environment elements during the red tide occurring in Haizhou bay. Adv. Mar. Sci. 27, 217–223.

Cui, B., Fei, D., Shao, G., Lu, Y., Chu, J., 2019a. Extracting raft aquaculture areas from remote sensing images via an improved U-net with a PSE structure. Rem. Sens. 11, 1–19. https://doi.org/10.3390/rs11172053.

Cui, J., Zhang, J., Monotilla, A.P., Huo, Y., Shi, J., Zhao, X., Kang, X., He, P., 2019b. Assessment of blooming Ulva macroalgae production potential in the Yellow Sea, China. Phycologia 58, 535–541. https://doi.org/10.1080/00318884.2018.1551016.

Cui, X., Li, S., Wang, X., Xue, X., 2019c. Driving factors of urban land growth in Guangzhou and its implications for sustainable development. Front. Earth Sci. 13, 464–477. https://doi.org/10.1007/s11707-018-0692-1.

Engle, C.R., 2016. Sustainable growth of aquaculture: the need for research to evaluate the impacts of regulatory frameworks. J. World Aquacult. Soc. 47, 461–463. https://doi.org/10.1111/jwas.12340.

Fan, J., Zhao, J., Song, D., Wang, Xinxin, Wang, Xiang, Su, X., 2018. Marine floating raft aquaculture dynamic monitoring based on multi-source GF imagery. In: 2018 7th International Conference on Agro-Geoinformatics. Agro-Geoinformatics. https://doi.org/10.1109/Agro-Geoinformatics.2018.8476085, 2018 1–4.

Hao, Y., Guan, C., Hou, C.Z., Tang, X.X., Wang, Y., 2021. Structural change of green macroalgal community attached on rafts in subei shoal and its correlation with environmental factors. Oceanol. Limnol. Sinica 52, 123–131. https://doi.org/10.11693/hyhz20200400111.

Huang, S., Xu, W., Xiong, Y., Wu, C., Dai, F., 2021. Combining textures and spatial features to extract tea plantations based on object-oriented method by using multispectral image. Spectrosc. Spectr. Anal. 41, 2565–2571.

Huo, Y., Zhang, J., Chen, L., Hu, M., Yu, K., Chen, Q., He, Q., He, P., 2013. Green algae blooms caused by Ulva prolifera in the southern Yellow Sea: identification of the original bloom location and evaluation of biological processes occurring during the early northward floating period. Limnol. Oceanogr. 58, 2206–2218. https://doi.org/10.4319/lo.2013.58.6.2206.

Jiang, P., Zhao, J., 2018. Identification of floating ecotype of ulva prolifera: implication for the green tide in the yellow sea. Oceanol. Limnol. Sinica 49, 959–966. https://doi.org/10.11693/hyhz20180800199.

Jiangsu Laver Association. In 2012, the Production Situation of Laver in Jiangsu Was Severe, and the Breeders Called for the Study of Countermeasures as Soon as Possible. http://www.bbwfish.com (accessed 21 October 2022).

Journal of the history of Lianyungang network. Lianyungang marine economic development. http://www.lygsz.gov.cn/. (Accessed 7 March 2022).

Kang, J., Sui, L., Yang, X., Liu, Y., Wang, Z., Wang, J., Yang, F., Liu, B., Ma, Y., 2019. Sea surface-visible aquaculture spatial-temporal distribution remote sensing: a case study in Liaoning Province, China from 2000 to 2018. Sustainability 11, 7186. https://doi.org/10.3390/SU11247186.

Kim, D., 2013. The relationship between climatic and oceanographic factors and laver aquaculture production. The Journal of Fisheries Business Administration 44, 77–84. https://doi.org/10.12939/fba.2013.44.3.077.

Li, F., 2016. The Research of Interregional Industry Transfer's Effect on Employment in China. Capital University Of Economics And Business.

Li, Y., Song, W., Xiao, J., Wang, Z., Fu, M., Zhu, M., Li, R., Zhang, X., Wang, X., 2014. Tempo-spatial distribution and species diversity of green algae micro-propagules in the Yellow Sea during the large-scale green tide development. Harmful Algae 39, 40–47. https://doi.org/10.1016/j.hal.2014.05.013.

Li, Y., Wang, Q., Li, X., Zhang, X., Zhang, Y., Chen, A., He, Q., Huang, Q., 2017. Unsupervised detection of acoustic events using information bottleneck principle. Digit. Signal Process.: A Review Journal 63, 123–134. https://doi.org/10.1016/j.dsp.2016.12.012.

Li, H., Xu, F., Weng, X., 2020. Recognition method for high-resolution remote-sensing imageries of ionic rare earth mining based on object-oriented technology. Arabian J. Geosci. 13 https://doi.org/10.1007/s12517-020-06104-0.

Liu, X., 2013b. Method to extract raft-cultivation area based on SPOT image. Sci. Surv. Mapp. 38, 41–43. https://doi.org/10.16251/j.cnki.1009-2307.2013.02.033.

Liu, D., Keesing, J.K., He, P., Wang, Z., Shi, Y., Wang, Y., 2013. The world's largest macroalgal bloom in the Yellow Sea, China: formation and implications. Estuarine. Coastal and Shelf Science 129, 2–10. https://doi.org/10.1016/j.ecss.2013.05.021.

Liu, X., Wang, Z., Zhang, X., 2016. A review of the green tides in the Yellow Sea, China. Mar. Environ. Res. 119, 189–196. https://doi.org/10.1016/j.marenvres.2016.06.004.

Liu, B., Chen, X., Zhang, Y., 2020. Influence of regular wave and ship characteristics on mooring force prediction by data-driven model. China Ocean Eng. 34, 589–596. https://doi.org/10.1007/s13344-020-0053-1.

Liu, C., Jiang, T., Zhang, Z., Sui, B., Pan, X., Zhang, L., Zhang, J., 2020a. Extraction method of offshore mariculture area under weak signal based on multisource feature fusion. J. Mar. Sci. Eng. 8, 1–13. https://doi.org/10.3390/jmse8020099.

Liu, Y., Wang, Z., Yang, X., Zhang, Y., Yang, F., Liu, B., Cai, P., 2020b. Satellite-based monitoring and statistics for raft and cage aquaculture in China's offshore waters. Int. J. Appl. Earth Obs. Geoinf. 91, 102118 https://doi.org/10.1016/j.jag.2020.102118.

Lu, Y., Li, Q., Du, X., Wang, H., Liu, J., 2015. A method of coastal aquaculture area automatic extraction with high spatial resolution images. Remote Sensing Technology and Application 30, 486–494.

Luo, M., Li, J., Hu, S., 2019. Exploring regional air quality evolution by developing a driving force model: case study of Beijing. J. Environ. Manag. 248, 109333 https://doi.org/10.1016/j.jenvman.2019.109333.

Luo, C., Qi, B., Liu, H., Guo, D., Lu, L., Fu, Q., Shao, Y., 2021. Using time series sentinel-1 images for object-oriented crop classification in google earth engine. Rem. Sens. 13, 1–19. https://doi.org/10.3390/rs13040561.

Nadarajah, S., Flaaten, O., 2017. Global aquaculture growth and institutional quality. Mar. Pol. 84, 142–151. https://doi.org/10.1016/j.marpol.2017.07.018.

Nadoushan, M.A., Alebrahim, A., 2017. Land use dynamics and landscape pattern changes in Khomeinishahr city , Iran. Indian Journal of Geo-Marine Sciences 46, 2361–2366.

Proisy, C., Viennois, G., Sidik, F., Andayani, A., Enright, J.A., Guitet, S., Gusmawati, N., Lemonnier, H., Muthusankar, G., Olagoke, A., Prosperi, J., Rahmania, R., Ricout, A., Soulard, B., Suhardjono, 2018. Monitoring mangrove forests after aquaculture abandonment using time series of very high spatial resolution satellite images: a case study from the Perancak estuary, Bali, Indonesia. Mar. Pollut. Bull. 131, 61–71. https://doi.org/10.1016/j.marpolbul.2017.05.056.

Quillien, N., Nordström, M.C., Guyonnet, B., Maguer, M., Le Garrec, V., Bonsdorff, E., Grall, J., 2015. Large-scale effects of green tides on macrotidal sandy beaches: habitat-specific responses of zoobenthos. Estuarine. Coastal and Shelf Science 164, 379–391. https://doi.org/10.1016/j.ecss.2015.07.042.

Song, H., Liu, L., Zhang, Y., Pe, S., 2017. Research on landscape pattern optimization of xianglan town based on GIS and fragstat. International Conference on Society Science 117. https://doi.org/10.2991/icoss-17.2017.39.

Sun, X., Du, H., Han, N., Ge, H., Gu, C., 2013. Multi-scale segmentation, object-based extraction of moso bamboo forest from SPOT5 imagery. Sci. Silvae Sin. 49, 80–87.

The Ministry of Agriculture of the People's Republic of China, 2020. Notice of the Ministry of agriculture on ''Printing and distributing the action plan for zero growth of fertilizer use by 2020'' and '' the action plan for zero growth of pesticide use by 2020. Gazette of the Ministry of Agriculture of the People's Republic of China 3, 19–27.

The National Marine Data Center. National science & technology resource sharing service platform of China. http://mds.nmdis.org.cn/. (Accessed 7 March 2022).

Wang, Z., Xiao, J., Fan, S., Li, Y., Liu, X., Liu, D., 2015. Who made the world's largest green tide in China? -an integrated study on the initiation and early development of the green tide in Yellow Sea. Limnol. Oceanogr. 60, 1105–1117. https://doi.org/10.1002/lno.10083.

Wen, L., Sun, M., Wu, M., 2021. Early warning method of sea area supervision based on faster R-CNN. J. Jilin Univ. (Sci. Ed.) 39, 421–429. https://doi.org/10.19292/j.cnki.jdxxp.20210407.001.

Xiao, F., Zhang, M., Guo, J., 2020. Research on land use classification based on landsat8 data and supervised classification method. Anhui Agricultural Science Bulletin 26, 110–113. https://doi.org/10.16377/j.cnki.issn1007-7731.2020.08.044.

Yan, X., Wang, S., 1993. The effexts of temperature, light intensity and aslinity on the decelopment of somatic cells from Porphyra haitanensis. Trop. Oceanol. 1, 84–99.

Yan, J., Zhao, S., Su, F., Du, J., Feng, P., Zhang, S., 2021. Tidal flat extraction and change analysis based on the rf-w model: a case study of jiaozhou bay, east China. Rem. Sens. 13, 1436. https://doi.org/10.3390/rs13081436.

Ying, Z., Wu, J., Del Valle, T.M., Yang, W., 2020. Spatiotemporal dynamics of coastal aquaculture and driving force analysis in Southeastern China. Ecosys. Health Sustain. 6 https://doi.org/10.1080/20964129.2020.1851145.

Zhang, X., Zhong, T., Huang, X., Jiang, H., Ding, X., 2013. Values of marine ecosystem services in Haizhou Bay. Sheng Tai Xue Bao/Acta Ecol. Sin. 33, 640–649. https://doi.org/10.5846/stxb201111221781.

Zhang, C., Li, X., Wu, M., Qin, W., Jun, Z., 2018a. Land cover information extraction in Kunyu Mountain Area Based on Landsat 8 oli data and object-oriented classification. Sci. Geogr. Sin. 38, 1904–1913. https://doi.org/10.13249/j.cnki.sgs.2018.11.018.

Zhang, Q., Yu, R., Chen, Z., Qiu, L., Wang, Y., Kong, F., Geng, H., Zhao, Y., Jiang, P., Yan, T., Zhou, M., 2018b. Genetic evidence in tracking the origin of Ulva prolifera blooms in the Yellow Sea, China. Harmful Algae 78, 86–94. https://doi.org/10.1016/j.hal.2018.08.002.

Zhang, G., Wu, M., Zhou, M., Zhao, L., 2020. The seasonal dissipation of Ulva prolifera and its effects on environmental factors: based on remote sensing images and field monitoring data. Geocarto Int. 9, 1–19. https://doi.org/10.1080/10106049.2020.1745301.

Zhang, C., Xiong, B., Li, X., Zhang, J., Kuang, G., 2021. Learning higher quality rotation invariance features for multioriented object detection in remote sensing images. IEEE J. Sel. Top. Appl. Earth Obs. Rem. Sens. 14, 5842–5853. https://doi.org/10.1109/JSTARS.2021.3085665.

Zhao, Y., 2003. In: first ed. Principles and Methods of Remote Sensing Application Analysis (Beijing, China).

Zheng, J., Yuan, G., Wei, A., Wang, C., Peng, M., 2021. Study on temporal and spatial distribution and eutrophication of nutrients in the northern area of Haizhou bay. Journal of Jiangsu Ocean University (Natural Science Edition) 30, 25–32.

Zou, L., Huang, S., 2015. Chinese aquaculture in light of green growth. Aquaculture Reports 2, 46–49. https://doi.org/10.1016/j.aqrep.2015.07.001.